Antimicrobial loading of nanotubular titanium surfaces favoring surface coverage by mammalian cells over bacterial colonization

Ren, Xiaoxiang; van der Mei, Henny C.; Ren, Yijin; Busscher, Henk J.; Peterson, Brandon W.

Published in:
Materials science & engineering c-Biomimetic and supramolecular systems

DOI:
10.1016/j.msec.2021.112021

Publication date:
2021

Materials Science & Engineering C 123 (2021) 112021

Contents lists available at ScienceDirect

Materials Science & Engineering C

journal homepage: www.elsevier.com/locate/msec

Antimicrobial loading of nanotubular titanium surfaces favoring surface coverage by mammalian cells over bacterial colonization

Xiaoxiang Ren [a], Henny C. van der Mei [a,*], Yijin Ren [b], Henk J. Busscher [a], Brandon W. Peterson [a]

[a] University of Groningen and University Medical Center of Groningen, Department of Biomedical Engineering, Antonius Deusinglaan 1, 9713 AV Groningen, the Netherlands

[b] University of Groningen and University Medical Center of Groningen, Department of Orthodontics, Hanzeplein 1, 9700 RB Groningen, the Netherlands

ARTICLE INFO

Keywords:
Silver nanoparticles
Co-cultures
Biomaterial-associated infection
Biomaterials implants
Local drug delivery
Gentamicin

ABSTRACT

Titanium is frequently used for dental implants, percutaneous pins and screws or orthopedic joint prostheses. Implant surfaces can become peri-operatively contaminated by surgically introduced bacteria during implantation causing lack of surface coverage by mammalian cells and subsequent implant failure. Especially implants that have to function in a bacteria-laden environment such as dental implants or percutaneous pins, cannot be surgically implanted while being kept sterile. Accordingly, contaminating bacteria adhering to implant surfaces hamper successful surface coverage by mammalian cells required for long-term functioning. Here, nanotubular titanium surfaces were prepared and loaded with Ag nanoparticles or gentamicin with the aim of killing contaminating bacteria in order to favor surface coverage by mammalian cells. In mono-cultures, unloaded nanotubules did not cause bacterial killing, but loading of Ag nanoparticles or gentamicin reduced the number of adhering *Staphylococcus aureus* or *Pseudomonas aeruginosa* CFUs. A gentamicin-resistant *Staphylococcus epidermidis* was only killed upon loading with Ag nanoparticles. However, unlike low-level gentamicin loading, loading with Ag nanoparticles also caused tissue-cell death. In bi-cultures, low-level gentamicin-loading of nanotubular titanium surfaces effectively eradicated contaminating bacteria favoring surface coverage by mammalian cells. Thus, care must be taken in loading nanotubular titanium surfaces with Ag nanoparticles, while low-level gentamicin-loaded nanotubular titanium surfaces can be used as a local antibiotic delivery system to negate failure of titanium implants due to peri-operatively introduced, contaminating bacteria without hampering surface coverage by mammalian cells.

1. Introduction

Nanostructured surfaces are called “promising” to control bacterial adhesion and biofilm formation and can be distinguished based on periodic- or random-occurrence of nanostructured features [1]. Nanostructured surfaces generally yield low bacterial adhesion and those bacteria that adhere have multiple contact sites with a substratum surface. Accordingly, bacteria adhering to nanostructured surfaces suffer highly localized cell wall deformation and sometimes even rupture causing bacterial death upon adhesion to sharp contact points [2,3]. Other promising features of nanostructured surfaces include thermal effects [4], photo-induced reactive oxygen species production [5] and increased antimicrobial housing [6]. Nanotubular titanium surfaces constitute an example of a highly periodic nanostructured surface with a high housing capacity for therapeutic agents, including antimicrobials and can be easily fabricated via electrochemical anodization [7].

Many biomaterials implants and devices, such as dental implants, percutaneous pins and screws or orthopedic joint prostheses, are made of titanium or its alloys and prone to failure due to colonization by infecting bacteria [3,8]. An immune system frustrated by the presence of the biomaterial [9], the biofilm mode of growth limiting deep penetration of an antimicrobial in the infectious biofilm [10] and an increasing number of bacterial strains and species that are resistant to all known antibiotics [11], have made infection the number one cause of biomaterials implant failure [12]. Antimicrobial-loaded nanotubular titanium surfaces might be ideally suitable to combat frequently occurring titanium-associated infection. Highly periodic nanotubular titanium surfaces have been loaded mainly with Ag nanoparticles (NPs)

* Corresponding author at: Department of Biomedical Engineering, University Medical Center Groningen, Antonius Deusinglaan 1, 9713 AV Groningen, the Netherlands.

E-mail address: h.c.van.der.mei@umcg.nl (H.C. van der Mei).

https://doi.org/10.1016/j.msec.2021.112021
Received 6 December 2020; Received in revised form 17 February 2021; Accepted 4 March 2021
Available online 10 March 2021

[13–22] over a loading range between 1.6 and 15.1 at.% Ag by X-ray photoelectron spectroscopy (XPS) [19,22] up to 14.9 wt% by Energy Dispersive X-ray Spectroscopy (EDS) [17]. In order to better control the loading process of nanotubes, nanotubes have also been loaded with Ag nanoparticles incorporated in polydopamine (PDA) [23]. The joint effect of cell wall damage by nanotube edges and dopamine-incorporated Ag nanoparticles at a loading of 0.4–1.6 at.% Ag yielded killing of Gram-positive *Staphylococcus aureus* and Gram-negative *Escherichia coli* [24]. Integration by tissue cells yields the best, natural protection of a biomaterials implant against colonizing bacteria [12,25]. This dictates that antimicrobial loaded nanotubular titanium surfaces should be tissue compatible, but reports on tissue compatibility of nanotubular titanium surfaces differ. Nanotubular titanium surfaces loaded with 4.1–4.9 at.% [21] or around 1.3 wt% [26] Ag nanoparticles stimulated proliferation of osteoblasts. Other studies report a negative impact on viability of human mesenchymal-stem cells [17] and osteoblast [20] over a Ag nanoparticle loading range of 3.3–14.5 at.% [18] or around 9.7 wt% [17].

Nanotubular titanium surfaces loaded with Ag nanoparticles (no loading level given) in combination with systemically administered vancomycin, rifampin, gentamicin or levofloxacin, enhanced antibiotic efficacy against an *S. aureus* infection in the medullary cavity underneath the tibia plateau in rats [27]. Insertion of a titanium rod with Ag nanoparticles filled nanotubules in combination with systemic application of antibiotics was demonstrated to yield synergistic efficacy against the infection, as supported by histological and immunohistochemical analyses, but not by culturing, i.e. the gold standard in clinical microbiology [28]. Moreover, gentamicin e.g., was daily administered by tail vein injection at a dose of 5 mg/kg every 24 h, which is at the limit of safe veterinary application in rodents [29] and humans (3–5 mg/kg every 24 h [30]). Although the study concludes that combination of Ag loaded nanotubular titanium with systemically applied gentamicin may be promising for the treatment of biomaterial-associated infection, systemically applied gentamicin can have severe side-effects [31] due to its oto- and nephrotoxicity [32]. Yet, gentamicin remains ideal for local delivery of an antibiotic and is clinically applied in bone cements and porous beads [31,33] for anchoring of titanium implants in bone for the treatment of osteomyelitis, respectively. Accordingly, nanotubular titanium surfaces have been loaded with different antibiotics [34], including gentamicin [35]. Commercial and clinically applied, gentamicin loaded bone cements have clinically safe, initial gentamicin release rates of around 5 μg/(cm^2 h) [36]. These clinically approved release rates are much lower than gentamicin release rates from experimental, gentamicin loaded nanotubular titanium surfaces, ranging from 15 to 212 μg/(cm^2 h) [35,37–39] to a potentially harmful value of 1060 μg/(cm^2 h) [39]. Although these high level loaded nanotubular titanium surfaces have been demonstrated to kill adhering bacteria [35,37–39], these high-level loadings may block the pathway of gentamicin loaded nanotubular titanium surfaces towards clinical translation by hampering tissue integration and due to the oto- and nephrotoxicity of gentamicin. Ideally, release rates should be restricted to the same rates as clinically occurring from e.g. gentamicin loaded bone cements.

Tissue integration and bacterial colonization are two simultaneous, competing processes that have been pictured as a “race for the surface” [25]. During surgical implantation, it is hard to avoid bacterial contamination of an implant surface [40]. This makes peri-operative contamination one of the pathways through which biomaterial-associated infection can develop [41]. Particularly, dental implants and percutaneous pins that have to be placed, heal and function in a bacteria-laden environment, are prone to peri-operative bacterial contamination and especially dental implants require effective surface coverage by mammalian cells for long-term functioning. This makes it imperative to study antimicrobial coatings in bi-culture models [42] in which surface coverage by mammalian cells is studied on bacterially contaminated surfaces (see Fig. 1), in addition to mono-culture studies on either bacterial killing or surface coverage by mammalian cells.

Therefore, we here first compare the effects of Ag nanoparticle or gentamicin loading of nanotubular titanium surfaces with respect to the killing of three frequently occurring clinical implant pathogens (*S. aureus*, *Staphylococcus epidermidis* (gentamicin-resistant) and *Pseudomonas aeruginosa*) and the adhesion, spreading and growth of human gingival fibroblasts and osteoblasts in mono-cultures. Antimicrobial loadings that passed mono-culture evaluations with a positive outcome, were subsequently evaluated in bi-cultures, in which mammalian cell adhesion, spreading and growth were evaluated in the presence of contaminating implant pathogens adhering to the surface (peri-operative infection model).

2. Materials and methods

2.1. Preparation of nanotubular arrays on a titanium surface and Ag nanoparticle loading

Titanium discs (14 mm of diameter, 1 mm in thickness, 99.6% purity, Alfa Aesar, Ward Hill, MA, USA) were degreased in methanol (99%), acetone (99%) and absolute ethanol using an ultrasonic cleaner for 10 min and subsequently rinsed in demineralized water. In order to equip the titanium discs with a nanotubular array, discs were anodized in an ethylene glycol solution (>99.5%) containing NH_4F (0.3 wt%) and H_2O (2 wt%) for 1 h at 30 V. Titanium foil was used as the anode and a platinum electrode was used as the cathode. The two electrodes were

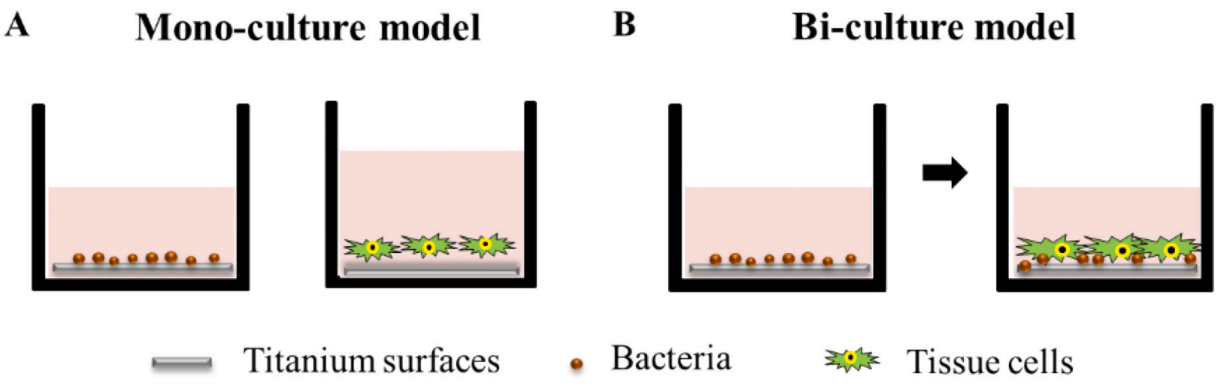

Fig. 1. Schematic presentation of the in vitro mono- and bi-culture models used to evaluate the impact of antimicrobial-loaded, nanotubular titanium surfaces on colonization by contaminating bacteria and surface coverage by mammalian cells. (A) Schematic presentation of the mono-culture bacterial (left) and mammalian cell (right) models used. (B) Schematic presentation of a peri-operative bi-culture model, in which a bacterially contaminated implant surface (left) is subsequently exposed to mammalian cells for adhesion and spreading on the surface (right).

separated at a distance of 4.5 cm. During the electrochemical process, the solution was stirred at 450 rpm. After anodizing, nanotubular titanium (Ti NT) discs were rinsed in demineralized water to remove possible residues of the electrolyte solution.

To introduce a polydopamine layer onto the surface of the nanotubular titanium discs, the discs were immersed in 2 mg/mL dopamine hydrochloride (Sigma-Aldrich, St. Louis, MO) (10 mM Tris buffer, pH 8.5), followed by shaking for 18 h. These discs were labeled as Ti NT-PDA. Subsequently, Ti NT-PDA discs were immersed in 1 mM $AgNO_3$ solutions (Sigma-Aldrich, St. Louis, MO, USA) during 6 h to allow reaction of $AgNO_3$ with PDA and form Ag nanoparticles in the nanotubules. The discs obtained were labeled as Ti NT-PDA-Ag discs. Alternatively, nanotubular titanium discs were immersed in a 1 mM $AgNO_3$ solution for 6 h and then immersed in 2 mg/mL dopamine hydrochloride, followed by shaking for 18 h. The obtained samples were labeled as Ti NT-Ag-PDA.

2.2. Loading of titanium samples with gentamicin

Gentamicin (G) was introduced either onto the surface of Ti, Ti NT or Ti NT-PDA discs. To this end, discs were immersed in 1 mL of a 200 μg/mL gentamicin solution (Sigma-Aldrich, St. Louis, MO, USA) for 2 h under gentle shaking. After 2 h, the samples were taken out carefully and washed with demineralized water. These discs were labeled as Ti-G, Ti NT-G and Ti NT-PDA-G.

2.3. Characterization of different titanium surfaces

Field emission scanning electron microscopy (Lyra FIB-SEM dual-beam, Tescan, Brno, Czechia) was used to observe the topography of the nanotubular structure. Energy dispersive X-ray spectroscopy (EDS) was done on the same microscope to analyze the chemical composition of the different titanium samples.

Water contact angles were measured using 1–1.5 μL water droplets. Water droplets were applied to the surfaces with a micro-syringe and contact angles derived from the droplet contours after black-white thresholding and analyzed using MATLAB software.

For X-ray photoelectron spectroscopy (XPS), a Surface Science instrument (Mountain View, CA, USA), equipped with an aluminum anode (10 kV, 22 mA) and a quartz monochromator was applied. The angle of photoelectron collection was 55° with the sample surfaces and the electron flood gun was set at 14 eV. A wide-scan over a binding energy range of 1–1200 eV was made with a 1000 × 250 μm spot and a pass energy of 150 eV. Binding energies were determined by setting the binding energy of the C_{1s} peak (carbon bound to carbon) at 284.8 eV. XPS was carried out in duplicate on two independently prepared samples of each titanium surface.

2.4. Measurement of the amount of gentamicin loaded and released

Gentamicin loading and release were measured using complexing of gentamicin with o-phthaldialdehyde [43]. First o-phthaldialdehyde reagent was prepared by mixing 2.5 g o-phthaldialdehyde (OPA), 62.5 mL methanol and 3 mL 2-mercaptoethanol to 560 mL 0.04 M sodium borate solution. The reagent was stored in a brown bottle in a dark chamber and settled for at least 24 h before use. The amount of gentamicin loaded was determined from the amount of residual gentamicin in solution. To this end, 1 mL of the gentamicin solution left after loading of a sample was mixed with 1 mL of OPA reagent and 1 mL isopropanol for 45 min. UV–Vis absorbance at 333 nm of the gentamicin-OPA complexes in the different solutions was measured to determine amounts of gentamicin loaded using a calibration curve over the concentration range between 1 and 200 μg/mL (Fig. S1).

Alternatively, gentamicin loaded discs were immersed in 1 mL of phosphate buffered saline (PBS, 10 mM potassium phosphate, 0.15 M NaCl, pH 7) with gently shaking to allow 24 h and 48 h release of gentamicin and the gentamicin concentrations determined as described above.

.

2.5. Antibacterial assays in mono-cultures

S. aureus ATCC 12600, *P. aeruginosa* ATCC 27853 and gentamicin-resistant *S. epidermidis* ATCC 35984 were used in this study to assess the antibacterial effect of the modified titanium samples. The minimum inhibitory concentration (MIC) of these strains to gentamicin amounted 1 μg/mL, 2 μg/mL, and 32 μg/mL, respectively. The bacteria were inoculated onto blood agar plates and incubated at 37 °C. After 24 h, one colony was transferred in 10 mL of Tryptone Soya Broth (TSB, OXOID, Basingstoke, UK) and incubated for 24 h at 37 °C. Subsequently, this bacterial pre-culture was added to 200 mL growth medium and incubated for another 16 h at 37 °C. Then, bacteria were harvested by centrifugation at 6500*g* for 5 min at 10 °C and washed twice with sterile PBS and suspended in PBS. Finally, the staphylococcal suspension was sonicated, while cooling in an ice bath (3 × 10 s at 30 W) in order to break bacterial aggregates. Bacterial suspensions were enumerated in a Bürker-Türk counting chamber and further diluted in PBS to a concentration of 5×10^6 bacteria/mL.

Antibacterial efficacy was measured using a membrane damage assay, based on SYTO 9 and propidium iodide (Thermo Fisher Scientific, Waltham, MA) staining and a culture-based assay. To allow initial bacterial adhesion, 1 mL of the bacterial suspension in PBS (5×10^6/mL) was put on the sample discs for bacterial sedimentation, after which the suspension was replaced by TSB and adhering bacteria were grown for 24 h at 37 °C. After 24 h, the culture medium was removed, and the discs were rinsed with PBS. 10 μL of a SYTO 9 solution and 10 μL of a propidium iodide solution were mixed in 7 mL PBS to stain the biofilm adhering to the discs. After staining for 15 min at room temperature in the dark, the staining solution was removed and bacteria were imaged using fluorescence microscopy (Leica DM4000, Leica Microsystems Ltd., Wetzlar, Germany) to visualize cell wall damaged bacteria.

To observe killing of bacteria on the different surfaces, discs with adhering bacteria, were placed in a 3M™ Petrifilm® Rapid Aerobic Count (RAC) Plate (3 M Microbiology, St. Paul, Minnesota, USA). Before use, the nutrient loaded gel side of the Petrifilm® was hydrated with 1 mL of sterilized demineralized water for 60 min. Next 10 μL of a bacterial suspension in PBS (5×10^6 bacteria/mL) was placed onto the disc surface and the disc was placed in the Petrifilm® system to contact the nutrient loaded gel. After incubation at 37 °C for 48 h, the numbers of colony forming units (CFUs) were enumerated. Killing efficacy was expressed with respect to the number of CFUs observed on uncoated, smooth titanium discs.

2.6. Surface coverage of titanium surfaces by HGFs and U2OS osteoblasts in mono-cultures

Human gingival fibroblasts (HGF) (HGF-1, ATCC-CRL-2014) and U2OS osteosarcoma cells (ATCC HTB-94) were obtained from the American Type Culture Collection (Manassas, USA) and grown in Dulbecco's modified Eagle's medium (DMEM-HG) supplemented with 10% Fetal Bovine Serum (FBS, Invitrogen, Breda, The Netherlands) at 37 °C in 5% CO_2. Cells from passages 5–10 were used. HGFs (1 mL, 2×10^4/mL) and U2OS cells (1 mL, 5×10^4/mL) were seeded on the different disc surfaces in a 24 well-plate and incubated at 37 °C in 5% CO_2. After 24 h of growth, the cells were stained with phalloidin-TRITC and DAPI and analyzed using a fluorescent microscope (Leica DM4000). Surface coverage and number of cells were subsequently derived from the images using image J software.

2.7. Surface coverage by mammalian cells upon bacterial challenges in bi-cultures

To mimic peri-operative contamination prior to surface coverage by mammalian cells, 1 mL of a *S. aureus*, *P. aeruginosa* or *S. epidermidis* suspension (5×10^4/mL) in PBS was added on the different discs in a 24 well-plate and bacteria allowed to sediment for 1 h. After 1 h, the discs were transferred to a new well, washed three times with PBS yielding approximately 1×10^3 bacteria/cm^2 on the implant surface and again transferred to a new well. Subsequently, 1 mL of a HGF (2×10^4/mL) or U2OS (5×10^4/mL) in DMEM-HG with FBS was added and incubated at 37 °C in 5% CO_2. After 24 h of growth, cells were stained and analyzed, as described above.

2.8. Statistical analyses

All data were plotted in GraphPad Prism and Origin. One-way ANOVA with a Bonferroni post-hoc test was employed using GraphPad Prism version 8.0 software. A value of $p < 0.05$ was deemed statistically significant.

3. Results

3.1. Characterization of nanotubular titanium surfaces with Ag nanoparticle loading

Uncoated titanium was relatively hydrophobic with a water contact angle of 62° (Fig. 2A). Application of nanotubular structures on the titanium surface enhanced the spreading of water and reduced water contact angles to between 20 and 22°, regardless of a PDA, PDA-Ag or Ag-PDA coating. Scanning electron microscopy revealed that the nanotubules were evenly distributed over the entire surface. After immersion in a $AgNO_3$ solution, nanotubules were preserved and clearly observable (Fig. 2B) possessing a diameter of 64 ± 10 nm. The diameters of the nanotubes became smaller after coating with polydopamine (55 ± 8 nm) and immersion in a $AgNO_3$ solution (Ti NT-PDA-Ag and Ti NT-Ag-PDA had diameters of 53 ± 8 nm and 52 ± 10 nm, respectively). EDS indicated that Ag was successfully applied (Table 1). Less Ag was measured in Ti NT-Ag-PDA (2.4 wt%) than in Ti NT-PDA-Ag (3.3 wt%). The depth of information of EDS is too high to detect the relatively thin oxide skin on the uncoated Ti surface. More surface sensitive XPS data (see Fig. S2, for wide-scan binding energy spectra) showed nearly identical elemental surface compositions for uncoated Ti and Ti NT surfaces. Ti and O occurred in a ratio of between 1:3 and 1:4, indicative of the presence of an oxide skin composed of different titanium oxides. Similar as in EDS, less Ag (only 0.5 at.%) was found in Ti NT-Ag-PDA than in Ti NT-PDA-Ag samples, possessing 2.7 at.% Ag (Table 2). Importantly, the high-resolution XPS spectra of Ti NT-Ag-PDA and Ti NT-PDA-Ag samples demonstrated an Ag binding energy peak with a gap of 6 eV in the 368.3 eV (Ag $3d_{5/2}$) and 374.3 eV (Ag $3d_{3/2}$) doublet (Fig. S2D), suggesting that metallic silver Ag(0) was formed [22].

Table 1
Elemental composition of the different titanium samples, determined using EDS and expressed both in weight and atom percentages.

Sample	Weight percentage (atom percentage)				
	C	N	O	Ti	Ag
Ti	7.0 (23.1)			93.0 (76.9)	
Ti NT			30.2 (56.5)	69.8 (43.5)	
Ti NT-PDA	9.5 (18.9)	3.2 (5.4)	32.4 (48.3)	55.0 (27.4)	
Ti NT-PDA-Ag	5.9 (12.6)	1.9 (3.4)	33.6 (53.7)	55.4 (29.6)	3.3 (0.8)
Ti NT-Ag-PDA	5.8 (12.6)	2.3 (4.4)	32.4 (52.5)	57.8 (31.6)	2.4 (0.6)
Ti-G	2.7 (7.4)	6.4 (14.8)	11.3 (23.0)	78.4 (53.3)	
Ti NT-G[a]	3.2 (7.2)	3.3 (6.3)	28.5 (47.4)	60.9 (33.9)	
Ti NT-PDA-G[a]	7.5 (15.1)	2.4 (4.1)	31.1 (46.6)	50.9 (25.5)	

[a] Trace amounts of Si, F, P, Na and K were found (not presented).

Table 2
Elemental composition of the different titanium surfaces, determined using XPS (see Fig. S2 for wide-scan binding energy spectra and high-resolution spectra of silver). Data represent averages with ± signs denoting SD over duplicate measurements with separately prepared samples.

Surface	Atom percentage[a]				
	C	N	O	Ti	Ag
Ti	26.7 ± 0.1	1.5 ± 0.2	51.7 ± 0.2	14.4 ± 0.0	
Ti NT	20.8 ± 2.2	0.5 ± 0.0	47.6 ± 4.5	16.7 ± 1.7	
Ti NT-PDA	52.7 ± 0.6	6.2 ± 0.1	30.5 ± 1.0	6.0 ± 0.8	
Ti NT-PDA-Ag	50.9 ± 1.3	5.7 ± 0.7	30.6 ± 0.9	6.1 ± 0.4	2.7 ± 0.4
Ti NT-Ag-PDA	55.4 ± 1.7	6.1 ± 0.1	29.8 ± 1.8	5.2 ± 0.5	0.5 ± 0.0
Ti-G	26.2 ± 2.4	2.9 ± 0.6	49.8 ± 6.7	14.4 ± 0.2	
Ti NT-G	24.4 ± 0.1	4.0 ± 0.7	46.4 ± 0.2	13.6 ± 0.6	
Ti NT-PDA-G	53.0 ± 1.4	6.1 ± 0.1	30.7 ± 0.2	6.4 ± 0.3	

[a] Trace amounts of Si, F, P, Ca were found (not presented).

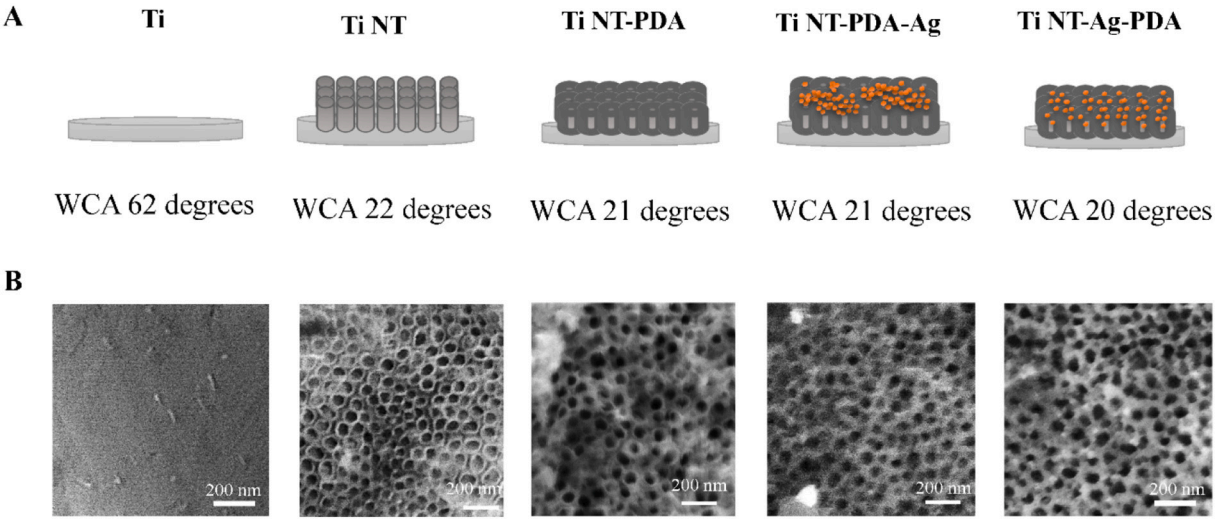

Fig. 2. Physicochemical characterization of different, AgNP loaded nanotubular titanium surfaces. (A) Schematics of the different nanotubular Ti surfaces together with their water contact angles (WCA). (B) SEM micrographs of the different titanium surfaces with and without nanotubules. The bright spots in the SEM of Ti NT-PDA-Ag represent AgNPs.

3.2. Gentamicin loading and release from different titanium surfaces

After the Ti, Ti NT and Ti NT-PDA discs were prepared, gentamicin was loaded on the samples by a simple immersion assay. Gentamicin loading showed a reduction in water contact angles to 20° both for Ti NT-G and Ti NT-PDA-G surfaces. In XPS binding energy spectra, gentamicin loading was evident by an increased N_{1s} signal (Table 2). A smooth titanium surface hardly adsorbed any gentamicin (Fig. 3A) compared with nanotubular titanium. Gentamicin loading of the Ti NT-PDA sample was less than in absence of PDA but still higher than of smooth titanium. In line, gentamicin release was highest from Ti NT-G surfaces (Fig. 3B). The increase in cumulative release between 24 and 48 h was relatively small compared to release over the first 24 h, indicating near-complete release of the gentamicin in around two days. Assuming an initially linear release kinetics over at least 24 h, it can be calculated that for our low-level gentamicin loaded nanotubular titanium surface, the release rate varied between 0.20 μg/(cm^2 h) (Ti NT-G) and 0.13 μg/(cm^2 h) (Ti NT PDA-G). These release rates are at the lower end of the gentamicin loading ranges observed in the literature for nanotubular titanium surfaces [35,37–39] and lower than gentamicin release from clinically approved bone cements [36].

3.3. Antibacterial activity assays in mono-cultures

Fluorescence images of *S. aureus*, *P. aeruginosa* and *S. epidermidis* biofilms after 24 h of growth showed the adhesion of bacteria on different titanium samples (Fig. S3). Nanotubules did not cause demonstrable cell wall damage, but the incorporation of Ag nanoparticles and gentamicin clearly prevented growth of adhering *S. aureus* and *P. aeruginosa* and virtually no bacteria could be observed. For the gentamicin-resistant *S. epidermidis* only Ag nanoparticles could prevent the growth. Fluorescence images furthermore show that gentamicin release from smooth titanium surface is insufficient to cause demonstrable cell wall damage.

When bacteria were applied to the surfaces in low numbers, typical of peri-operative contamination, 48 h growth within the Petrifilm® plates yielded between 10^4 and 10^5 CFU/cm^2, neither application of nanotubules with or without PDA, nor gentamicin adsorption to smooth titanium surfaces caused a decrease in the viability of contaminating bacteria, regardless of the strain considered (Fig. 4). However, when Ti NT was loaded with gentamicin or Ag nanoparticles, bacterial killing was more than 3 log units for both *S. aureus* and *P. aeruginosa*. For the gentamicin-resistant *S. epidermidis* only loading with Ag nanoparticles showed killing of more than 4 log units. Ag nanoparticles covered with PDA (0.5 at.% Ag) were less effective in reducing the number of CFUs than when applied on top of an existing layer of PDA (2.7 at.% Ag).

3.4. Surface coverage of different coating surfaces by HGFs and U2OS cells in mono-cultures

Mammalian cells spread and adhered well on titanium surfaces, regardless of the presence of nanotubules with or without a PDA layer, both with respect to surface coverage for HGF and U2OS cells as well as with respect to cell numbers (Fig. 5). Despite its known oto- and nephrotoxicity [44], our low-level gentamicin loading had no negative effects on tissue spreading and adhesion, but loading with Ag nanoparticles (0.5 at.% and 2.7 at.% Ag) was detrimental over the two concentrations applied and caused a reduction in cell surface coverage to well below the critical limit of 40%, required for tissue cells to win the race for the surface from colonizing bacteria [45]. Therefore, Ag nanoparticle loading was not further pursued in bi-culture studies.

3.5. Surface coverage by mammalian cells on bacterially contaminated titanium surfaces in bi-cultures

In a peri-operative contamination model, the presence of *S. aureus* (Figs. S5A and S6A) or *P. aeruginosa* (Figs. S5B and S6B) adhering on titanium surfaces in absence of a gentamicin loading, led to a strongly reduced surface coverage and number of adhering HGFs (Fig. 6A and B for *S. aureus* and *P. aeruginosa*, respectively) and U2OS cells (Fig. 7A and B for *S. aureus* and *P. aeruginosa*, respectively) as compared with tissue cell spreading and adhesion on titanium surfaces without contaminating bacteria. Attesting to the relatively low virulence of *S. epidermidis* [46] and despite the gentamicin-resistance of the strain used, the presence of contaminating *S. epidermidis* (Figs. S5C and S6C) yielded no reductions in cell surface coverage or numbers (Figs. 6C and 7C for HGF and U2OS cells, respectively). Gentamicin loading of smooth titanium surfaces did not enhance spreading and adhesion of tissue cells on surfaces contaminated with *S. aureus* or *P. aeruginosa*. However, due to the increased gentamicin housing capacity of nanotubular titanium surfaces, tissue cell spreading and adhesion in presence of contaminating *S. aureus* or *P. aeruginosa* were enhanced to the same level as observed on uncontaminated titanium surfaces. Due to the low virulence of *S. epidermidis*, further improvement in cell surface coverage or numbers upon gentamicin loading was impossible. Importantly however in this case, gentamicin loading had no negative effects on surface coverage by mammalian cells.

4. Discussion

Titanium and its alloys are widely used as implant materials. However, around 10% failures of titanium implants result from bacterial infection within a year after implantation [47], presumably for a large

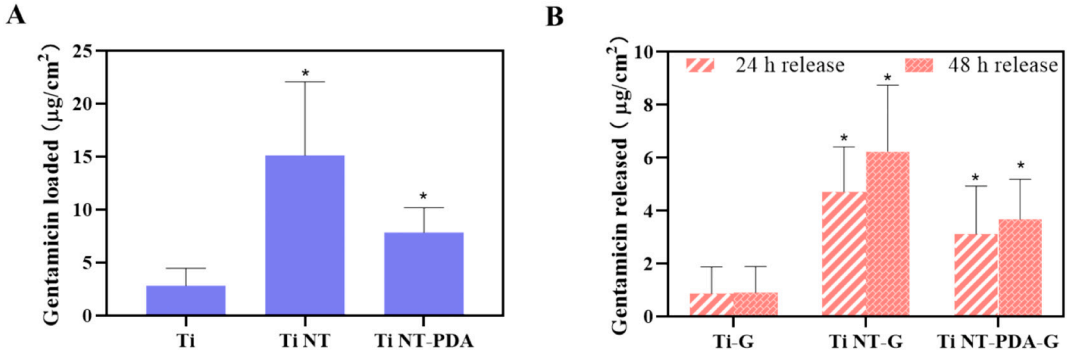

Fig. 3. Gentamicin loading and release from different nanotubular titanium surfaces.
(A) The amount of gentamicin loaded on smooth titanium surfaces (Ti) and in nanotubular titanium surfaces in absence (Ti NT) and presence of a PDA overlayer (Ti NT-PDA) after 2 h immersion in 1 mL (200 μg/mL) gentamicin solution. (B) The cumulative amount of gentamicin released from the different titanium surfaces after 24 h and 48 h immersion in 1 mL PBS solution. Error bars denote SEM over three experiments. * denotes a significant difference from smooth titanium samples ($p < 0.05$).

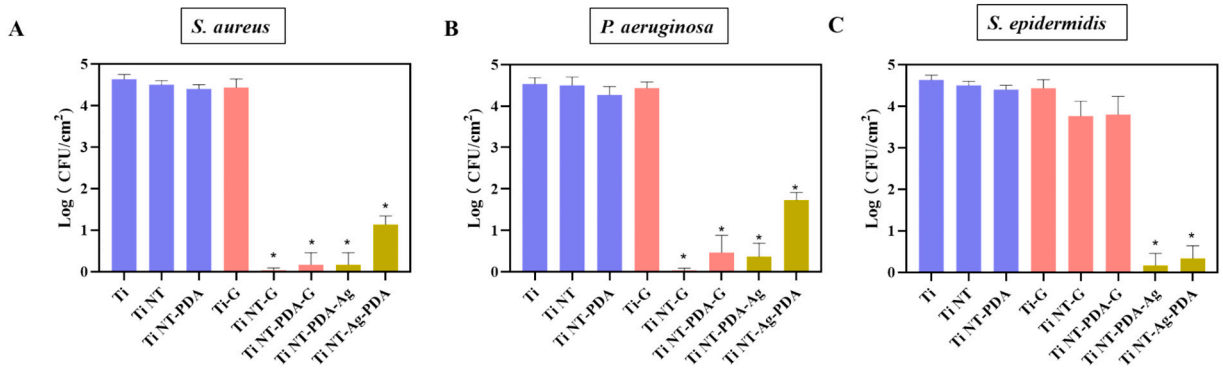

Fig. 4. Killing of contaminating bacteria growing on smooth and different antimicrobial-loaded, nanotubular titanium surfaces. (A) Numbers of *S. aureus* CFUs retrieved per unit surface area from the different titanium surfaces. (B) Same as panel (A), now for *P. aeruginosa*. (C) Same as panel (A), now for gentamicin-resistant *S. epidermidis*. Error bars denote SEM over three experiments with separately cultured bacteria. * denotes a significant difference from smooth titanium samples without antimicrobial loading ($p < 0.05$).

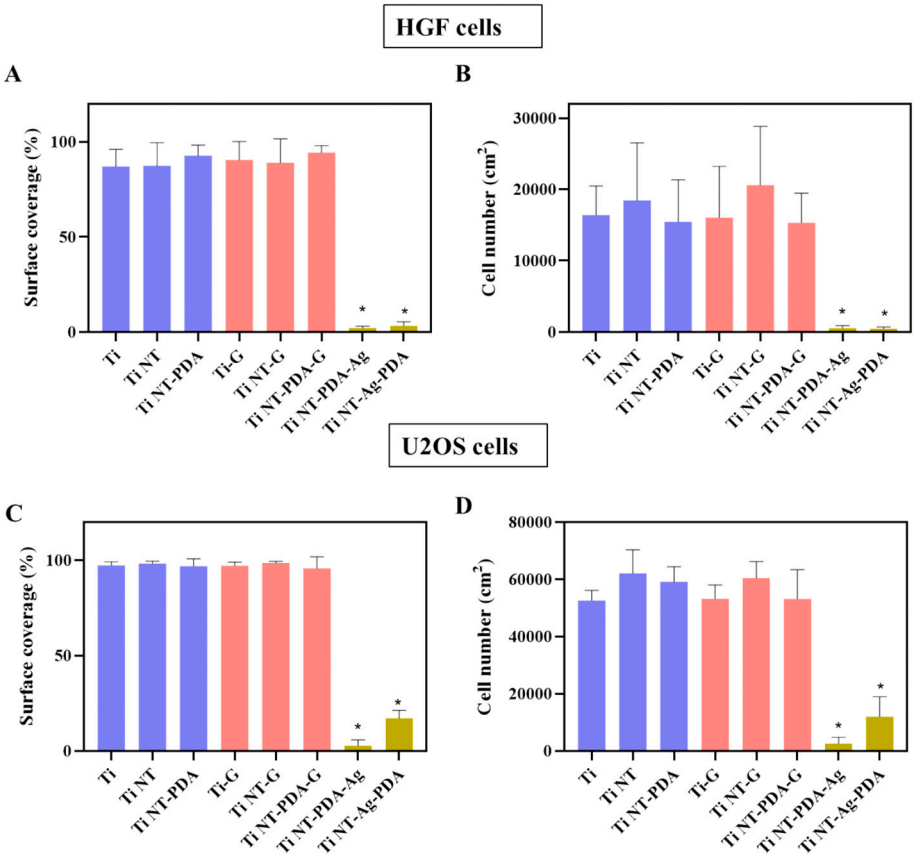

Fig. 5. Interaction of mammalian cells after 24 h of growth on smooth and different antimicrobial-loaded, nanotubular titanium surfaces (data represent a quantification of the fluorescence images presented in Fig. S4). (A) Surface coverage by adhering HGFs after growth on the different titanium surfaces. (B) Number of adhering HGFs (per cm^2) after growth on the different titanium surfaces. (C) Same as panel (A), now for U2OS cells. (D) Same as panel (B), now for U2OS cells. Error bars denote SEM over three experiments with separately cultured cells. * denotes a significant difference from smooth titanium surfaces without antimicrobial loading ($p < 0.05$).

part due to peri-operative bacterial contamination. Ag nanoparticle or gentamicin loaded nanotubular titanium surfaces have been described to discourage infectious biofilm formation of titanium surfaces, but often without consideration of clinical constraints or collateral damage to tissue cells surrounding an implant. Literature studies report effective killing of bacteria on nanotubular surfaces at high-levels (up to 14.9 wt %) of Ag nanoparticle loading [18,20,22], while we here demonstrate (Tables 1 and 2) that loading (up to 3.3 wt%) suffices for killing of bacteria adhering to titanium surfaces in numbers typical of peri-operative contamination [48]. Previously, Ag nanoparticle loading of nanotubular titanium surfaces has also been described to kill pathogenic *S. aureus* and *E. coli* [24]. Unfortunately, we found severe reductions in surface coverage by HGF and U2OS cells and numbers even upon Ag nanoparticle loading of nanotubular titanium surfaces (Fig. 5). Literature has been conflicting with regards to effects of Ag nanoparticle loading of nanotubular titanium surfaces [18,20,22,49,50]. Based on our results of Ag nanoparticle loading of nanotubular titanium surfaces, we decided that the combined effects of nanotubular titanium and loading of nanotubules with Ag nanoparticles is too damaging towards mammalian cells covering the surface to make it suitable as a coating for biomaterials implants.

Literature also described, that high-level loading of nanotubular titanium surfaces with gentamicin yielded killing of several pathogenic bacterial strains, but gentamicin release rates were extremely high around 133–1060 μg/(cm^2 h) [38,39]. Mostly, these gentamicin concentrations have not been reported to present a negative impact on

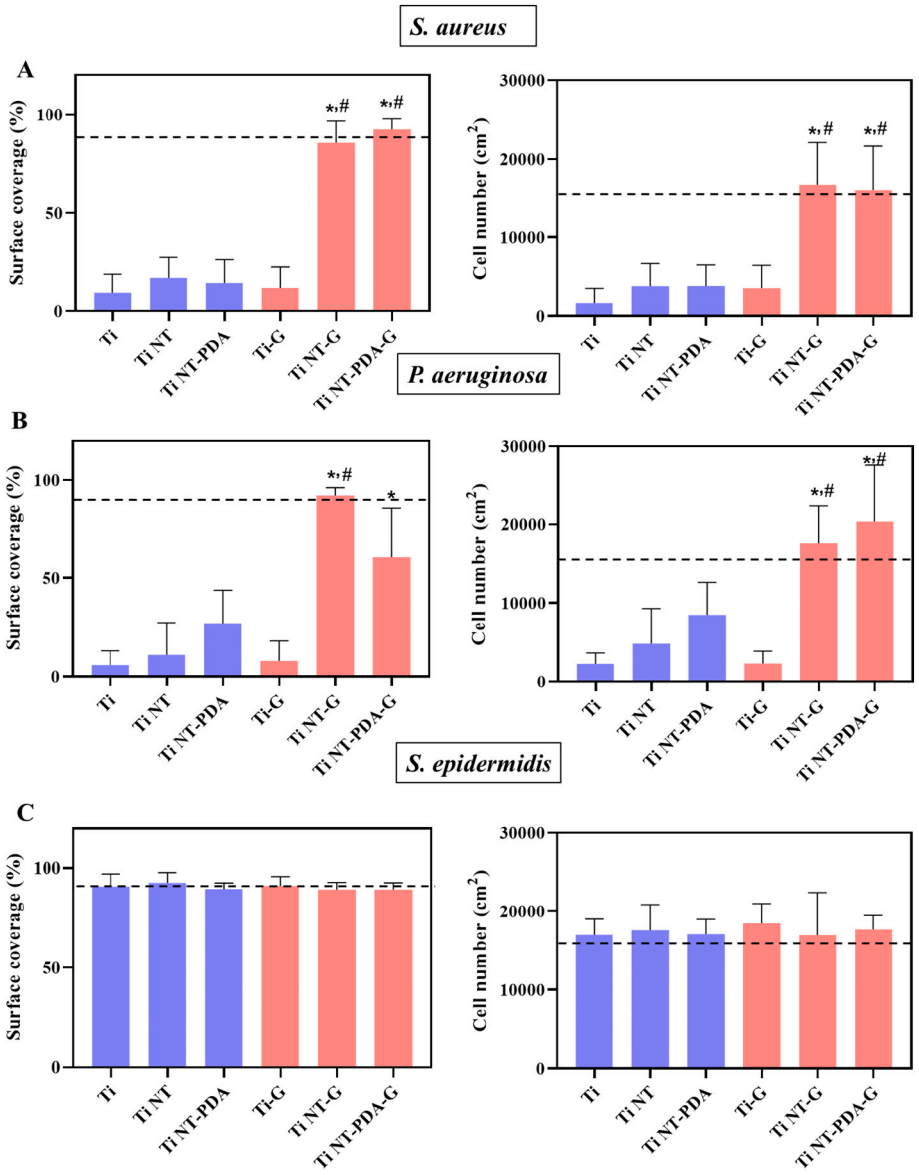

Fig. 6. The race for the surface: growth of HGF cells on different, bacterially contaminated nanotubular titanium surfaces with and without gentamicin-loading (peri-operative contamination model). Contaminating bacteria were sedimented from suspension, yielding approximately 1×10^3 bacteria/cm^2 (data represent a quantification of the fluorescence images presented in Fig. S5). (A) Percentage surface coverage of a substratum surface by adhering HGF and the number of adhering HGF (per cm^2) in absence (dotted line) and presence of *S. aureus* contaminated surfaces. (B) Same as panel (A), now for *P. aeruginosa* contaminated surfaces. (C) Same as panel (A), now for surfaces contaminated by a gentamicin-resistant *S. epidermidis* strain. The dotted lines indicate the percentage surface coverage and number of cells per cm^2 of a smooth titanium surface in absence of bacterial contamination. Error bars denote SEM over three experiments with separately cultured bacteria and tissue-cells. * denotes a significant difference from smooth titanium surface, while # indicates a significant difference from corresponding titanium surfaces without antimicrobial loading ($p < 0.05$).

mammalian cell behavior [35,37,39], although few papers did report a negative impact of high-level gentamicin loading of nanotubular titanium surfaces on osteoblast cells [51]. In general unfortunately, the in vitro evaluations applied [35,37–39] and their results, negate the clinical observations of oto- and nephrotoxicity of gentamicin. Therefore, our work is uniquely based on low-level gentamicin loading, in which "low" is defined as yielding smaller or equal gentamicin release rates as from clinically-applied gentamicin loaded bone cements [36] used to fix titanium implants in bone. Approval of gentamicin loaded bone cement has been quite a struggle in the past between clinicians wanting to protect their patients against bacterial infections and regulatory bodies disapproving clinical use of gentamicin-loaded cements because of oto- and nephrotoxicity [52]. Particularly in the USA, the FDA has been lingering longest with the approval of gentamicin loaded bone cement. Based on recently published, so-called "enrichment principles" proposed by a Trans-Atlantic consortium [53], an already-approved combination of implants or devices with an antimicrobial coating, replacement of that coating with another coating or application to an implant or device with different designs or geometries should not require the same type and extent of regulatory assessment of risk/benefit as for the already approved device. By comparison with bone cement, this principle, called "enrichment-from-component", would be applicable to our low-level gentamicin loaded, nanotubular titanium surfaces and make its prospects for downward clinical translation more likely than of high-level gentamicin loaded variants.

Low-level gentamicin-loaded nanotubular titanium surfaces would be particularly useful as a prophylactic coating to prevent negative effects of peri-operatively introduced bacteria on a biomaterials implant surface because in presence of gentamicin loading the balance between surface coverage by mammalian cells and bacterial colonization is clearly shifted in favor of cell surface coverage.

5. Conclusions

Low-level loading of nanotubular titanium surfaces with gentamicin favors surface coverage by mammalian cells over colonization by peri-operatively introduced bacteria. Loading of nanotubular titanium with Ag nanoparticles should be avoided because of adverse effects on mammalian cells due to the combination of Ag nanoparticles and a nanostructured surface that together yield a negative impact of surface coverage by mammalian cells. This combination remains useful however to kill contaminating bacteria in applications of titanium in which

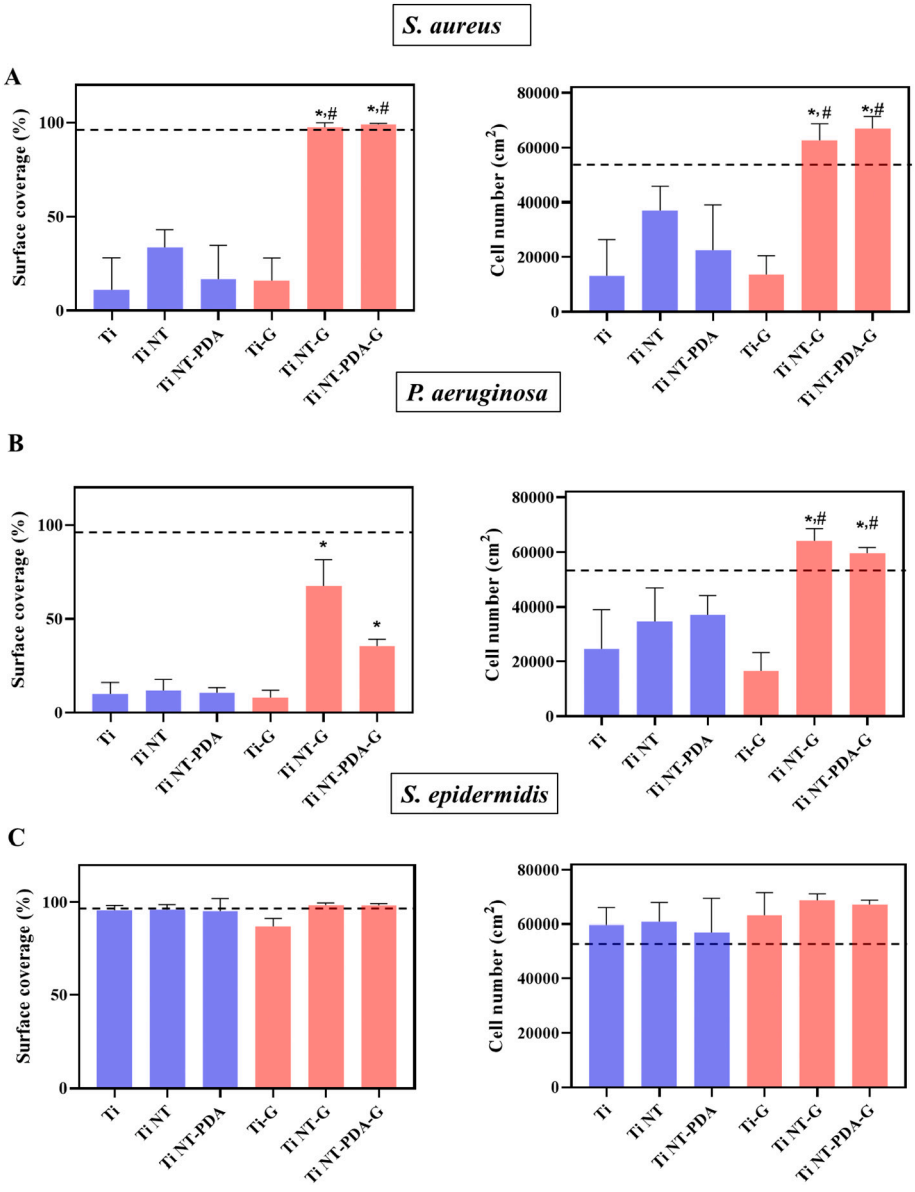

Fig. 7. The race for the surface: growth of U2OS cells on different, bacterially contaminated nanotubular titanium surfaces with and without gentamicin-loading (peri-operative contamination model). Contaminating bacteria were sedimented from suspension, yielding approximately 1×10^3 bacteria cm^{-2} (data represent a quantification of the fluorescence images presented in Fig. S6). (A) Percentage surface coverage of a substratum surface by adhering U2OS cells and the number of adhering U2OS cells (per cm^2) in absence (dotted line) and presence of *S. aureus* contaminated surfaces. (B) Same as panel (A), now for *P. aeruginosa* contaminated surfaces. (C) Same as panel (A), now for surfaces contaminated by gentamicin-resistant *S. epidermidis*. The dotted lines indicate the percentage surface coverage and number of cells per cm^2 of a smooth titanium surface in absence of bacterial contamination. Error bars denote SEM over three experiments with separately cultured bacteria and tissue-cells. * denotes a significant difference from smooth titanium surface, while # indicates a significant difference from corresponding titanium surfaces without antimicrobial loading ($p < 0.05$).

surface coverage by mammalian cells is not required.

CRediT authorship contribution statement

Conception and design of study: all authors
Acquisition of data: Xiaoxiang Ren
Analysis and interpretation of data: Xiaoxiang Ren, Henny C. van der Mei, Henk J. Busscher, Brandon W. Peterson
Drafting the manuscript: Xiaoxiang Ren, Brandon Peterson
Revising the manuscript: Henny C. van der Mei, Yijin Ren, Henk J. Busscher
Supervision: Brandon W. Peterson, Henny C. van der Mei, Henk J. Busscher
Approval final version of the manuscript: all authors.

Declaration of competing interest

The authors declare the following financial interests/personal relationships which may be considered as potential competing interests: HJB is also director-owner of a consulting company SASA BV. The authors declare no potential conflicts of interest with respect to authorship and/or publication of this article. Opinions and assertions contained herein are those of the authors and are not construed as necessarily representing views of the funding organizations or their employer(s).

Acknowledgements

XR likes to thank the China Scholarship Council and W.J. Kolff Institute, UMCG, Groningen, The Netherlands for financial support. Authors were employed by their own organizations.

Appendix A. Supplementary data

Supplementary data to this article can be found online at https://doi.org/10.1016/j.msec.2021.112021.

References

[1] Y. Luan, S. Liu, M. Pihl, H.C. van der Mei, J. Liu, F. Hizal, C.H. Choi, H. Chen, Y. Ren, H.J. Busscher, Bacterial interactions with nanostructured surfaces, Curr, Opin. Colloid Interface Sci. 38 (2018) 170–189.
[2] E.P. Ivanova, J. Hasan, H.K. Webb, V.K. Truong, G.S. Watson, J.A. Watson, V. A. Baulin, S. Pogodin, J.Y. Wang, M.J. Tobin, C. Löbbe, R.J. Crawford, Natural

bactericidal surfaces: mechanical rupture of *Pseudomonas aeruginosa* cells by cicada wings, Small 8 (2012) 2489–2494.
[3] Y. Cao, B. Su, S. Chinnaraj, S. Jana, L. Bowen, S. Charlton, P. Duan, N. S. Jakubovics, J. Chen, Nanostructured titanium surfaces exhibit recalcitrance towards *Staphylococcus epidermidis* biofilm formation, Sci, Rep. 8 (2018) 1071.
[4] M. Pihl, E. Bruzell, M. Andersson, Bacterial biofilm elimination using gold nanorod localised surface plasmon resonance generated heat, Mater. Sci. Eng. C 80 (2017) 54–58.
[5] D. Campoccia, L. Montanaro, C.R. Arciola, A review of the biomaterials technologies for infection-resistant surfaces, Biomaterials 34 (2013) 8533–8554.
[6] F. Hizal, I. Zhuk, S. Sukhishvili, H.J. Busscher, H.C. van der Mei, C.H. Choi, Impact of 3D hierarchical nanostructures on the antibacterial efficacy of a bacteria-triggered self-defensive antibiotic coating, ACS Appl. Mater. Interfaces 7 (2015) 20304–20313.
[7] S. Mei, H. Wang, W. Wang, L. Tong, H. Pan, C. Ruan, Q. Ma, M. Liu, H. Yang, L. Zhang, Y. Cheng, Y. Zhang, L. Zhao, P.K. Chu, Antibacterial effects and biocompatibility of titanium surfaces with graded Ag incorporation in titania nanotubes, Biomaterials 35 (2014) 4255–4265.
[8] C. Yue, B. Zhao, R. Kuijer, H.C. van der Mei, H.J. Busscher, E.T.J. Rochford, The implant infection paradox: why do some succeed when others fail? Eur. Cells Mater. 29 (2015) 303–313.
[9] B.N. Brown, S.F. Badylak, Expanded applications, shifting paradigms and an improved understanding of host-biomaterial interactions, Acta Biomater. 9 (2013) 4948–4955.
[10] D. Davies, Understanding biofilm resistance to antibacterial agents, Nat. Rev. Drug Discov. 2 (2003) 114–122.
[11] S.B. Levy, M. Bonnie, Antibacterial resistance worldwide: causes, challenges and responses, Nat. Med. 10 (2004) S122–S129.
[12] H.J. Busscher, H.C. van der Mei, G. Subbiahdoss, P.C. Jutte, J.J.A.M. van den Dungen, S.A.J. Zaat, M.J. Schultz, D.W. Grainger, Biomaterial-associated infection: locating the finish line in the race for the surface, Sci. Transl. Med. 4 (2012) 153rv10.
[13] L. Juan, Z. Zhimin, M. Anchun, L. Lei, Z. Jingchao, Deposition of Ag NP on titanium surface for antibacterial effect, Int. J. Nanomedicine 5 (2010) 261–267.
[14] K. Das, S. Bose, A. Bandyopadhyay, B. Karandikar, B.L. Gibbins, Surface coatings for improvement of bone cell materials and antimicrobial activities of Ti implants, J. Biomed. Mater. Res. - Part B Appl. Biomater. 87 (2008) 455–460.
[15] L. Liu, R. Cai, Y. Wang, G. Tao, L. Ai, P. Wang, M. Yang, H. Zuo, P. Zhao, H. He, Polydopamine-assisted silver nanoparticle self-assembly on sericin/agar film for potential wound dressing application, Int. J. Mol. Sci. 19 (2018) 2875.
[16] X. Ding, Y. Zhang, J. Ling, C. Lin, Rapid mussel-inspired synthesis of PDA-Zn-Ag nanofilms on TiO2 nanotubes for optimizing the antibacterial activity and biocompatibility by doping polydopamine with zinc at a higher temperature, Colloids Surfaces B Biointerfaces 171 (2018) 101–109.
[17] S. Amin Yavari, L. Loozen, F.L. Paganelli, S. Bakhshandeh, K. Lietaert, J.A. Groot, A.C. Fluit, C.H.E. Boel, J. Alblas, H.C. Vogely, H. Weinans, A.A. Zadpoor, Antibacterial behavior of additively manufactured porous titanium with nanotubular surfaces releasing silver ions, ACS Appl. Mater. Interfaces 8 (2016) 17080–17089.
[18] A.P.R. Alves Claro, R.T. Konatu, A.L. do A. Escada, M.C. de Souza Nunes, C. V. Maurer-Morelli, M.F. Dias-Netipanyj, K.C. Popat, D. Mantovani, Incorporation of Ag NP on Ti7.5 Mo alloy surface containing TiO2 nanotubes arrays for promoting antibacterial coating, *vitro* and *in vivo* study, Appl. Surf. Sci. 455 (2018) 780–788.
[19] L. Zhao, H. Wang, K. Huo, L. Cui, W. Zhang, H. Ni, Y. Zhang, Z. Wu, P.K. Chu, Antibacterial nano-structured titania coating incorporated with Ag NP, Biomaterials 32 (2011) 5706–5716.
[20] J. Chen, M.L. Mei, Q.L. Li, C.H. Chu, Mussel-inspired Ag-nanoparticle coating on porous titanium surfaces to promote mineralization, RSC Adv. 6 (2016) 104025–104035.
[21] M. Li, Q. Liu, Z. Jia, X. Xu, Y. Shi, Y. Cheng, Y. Zheng, Polydopamine-induced nanocomposite Ag/CaP coatings on the surface of titania nanotubes for antibacterial and osteointegration functions, J. Mater. Chem. B 3 (2015) 8796–8805.
[22] Z. Jia, P. Xiu, P. Xiong, W. Zhou, Y. Cheng, S. Wei, Y. Zheng, T. Xi, H. Cai, Z. Liu, C. Wang, W. Zhang, Z. Li, Additively manufactured macroporous titanium with silver-releasing micro-/nanoporous surface for multipurpose infection control and bone repair - a proof of concept, ACS Appl. Mater. Interfaces 8 (2016) 28495–28510.
[23] J. Xu, N. Xu, T. Zhou, X. Xiao, B. Gao, J. Fu, T. Zhang, Polydopamine coatings embedded with silver nanoparticles on nanostructured titania for long-lasting antibacterial effect, Surf, Coatings Technol. 320 (2017) 608–613.
[24] A. Gao, R. Hang, X. Huang, L. Zhao, X. Zhang, L. Wang, B. Tang, S. Ma, P.K. Chu, The effects of titania nanotubes with embedded silver oxide nanoparticles on bacteria and osteoblasts, Biomaterials 35 (2014) 4223–4235.
[25] A.G. Gristina, P.T. Naylor, Q.N. Myrvik, Biomaterial-centered infections: microbial adhesion versus tissue integration, Science 237 (1987) 1588–1595.
[26] M. Sarraf, A. Dabbagh, B. Abdul Razak, R. Mahmoodian, B. Nasiri-Tabrizi, H.R. M. Hosseini, S. Saber-Samandari, N.H. Abu Kasim, H. Abdullah, N.L. Sukiman, Highly-ordered TiO2 nanotubes decorated with Ag2O NP for improved biofunctionality of Ti6Al4V, Surf, Coatings Technol. 349 (2018) 1008–1017.
[27] N. Xu, H. Cheng, J. Xu, F. Li, B. Gao, Z. Li, C. Gao, K. Huo, J. Fu, W. Xiong, Ag-loaded nanotubular structures enhanced bactericidal efficiency of antibiotics with synergistic effect *in vitro* and *in vivo*, Int. J. Nanomedicine 12 (2017) 731–743.
[28] G.E. Pfyffer, H.M. Welscher, P. Kissling, C. Cieslak, M.J. Casal, J. Gutierrez, S. Rüsch-Gerdes, Comparison of the mycobacteria growth indicator tube (MGIT) with radiometric and solid culture for recovery of acid-fast bacilli, J. Clin. Microbiol. 35 (1997) 364–368.
[29] C. Chareul, J. Faccini, A. Monro, J. Nachbaur, A second peak in uptake of gentamicin by rat kidney after cessation of treatment, Biopharm. Drug Dispos. 5 (1984) 21–24.
[30] G. Kahlmeter, J.I. Dahlager, Aminoglycoside toxicity - a review of clinical studies published between 1975 and 1982, J. Antimicrob. Chemother. 13 (1984) 9–22.
[31] D. Neut, H. van de Belt, J.R. Van Horn, H.C. van der Mei, H.J. Busscher, The effect of mixing on gentamicin release from polymethylmethacrylate bone cements, Acta Orthop, Scand 74 (2003) 670–676.
[32] A. Lakhera, A. Ganeshpurkar, D. Bansal, N. Dubey, Chemopreventive role of *Coriandrum sativum* against gentamicin-induced renal histopathological damage in rats, Interdiscip, Toxicol. 8 (2015) 99–102.
[33] N. Müller, P. Schmidlin, M. Özcan, Adhesive durability of bone cements containing gentamicin or gentamicin/clindamycin-based antibiotics on titanium used for oral implants, J. Adhes. Sci. Technol. 30 (2016) 2130–2145.
[34] H. Zhang, Y. Sun, A. Tian, X. Xue, L. Wang, A. Alquhali, X. Bai, Improved antibacterial activity and biocompatibility on vancomycin-loaded TiO2 nanotubes: *in vivo* and *in vitro* studies, Int. J. Nanomedicine 8 (2013) 4379–4389.
[35] T. Kumeria, H. Mon, M.S. Aw, K. Gulati, A. Santos, H.J. Griesser, D. Losic, Advanced biopolymer-coated drug-releasing titania nanotubes (TNTs) implants with simultaneously enhanced osteoblast adhesion and antibacterial properties, Colloids Surfaces B Biointerfaces 130 (2015) 255–263.
[36] D. Neut, R.J.B. Dijkstra, J.I. Thompson, H.C. van der Mei, H.J. Busscher, Antibacterial efficacy of a new gentamicin-coating for cementless prostheses compared to gentamicin-loaded bone cement, J. Orthop. Res. 29 (2011) 1654–1661.
[37] W.T. Lin, H.L. Tan, Z.L. Duan, B. Yue, R. Ma, G. He, T.T. Tang, Inhibited bacterial biofilm formation and improved osteogenic activity on gentamicin-loaded titania nanotubes with various diameters, Int. Nanomedicin. 9 (20144) 1215–1230.
[38] W. Feng, Z. Geng, Z. Li, Z. Cui, S. Zhu, Y. Liang, Y. Liu, R. Wang, X. Yang, Controlled release behaviour and antibacterial effects of antibiotic-loaded titania nanotubes, Mater. Sci. Eng. C 62 (2016) 105–112.
[39] K.C. Popat, M. Eltgroth, T.J. LaTempa, C.A. Grimes, T.A. Desai, Decreased *Staphylococcus epidermidis* adhesion and increased osteoblast functionality on antibiotic-loaded titania nanotubes, Biomaterials 28 (2007) 4880–4888.
[40] A.D. Pye, D.E.A. Lockhart, M.P. Dawson, C.A. Murray, A.J. Smith, A review of dental implants and infection, J. Hosp. Infect. 72 (2009) 104–110.
[41] M. Abu-Ta'a, M. Quirynen, W. Teughels, D. Van Steenberghe, Asepsis during periodontal surgery involving oral implants and the usefulness of peri-operative antibiotics: a prospective, randomized, controlled clinical trial, J. Clin. Periodontol. 35 (2008) 58–63.
[42] G. Subbiahdoss, R. Kuijer, D.W. Grijpma, H.C. van der Mei, H.J. Busscher, Microbial biofilm growth vs. tissue integration: "the race for the surface" experimentally studied, Acta Biomater. 5 (2009) 1399–1404.
[43] X. Zhang, U.P. Wyss, D. Pichora, M.F.A. Goosen, Biodegradable controlled antibiotic release devices for osteomyelitis: optimization of release properties, J. Pharm. Pharmacol. 46 (1994) 718–724.
[44] R. Reimschuessel, D. Williams, Development of new nephrons in adult kidneys following gentamicin-induced nephrotoxicity, Ren, Fail. 17 (1995) 101–106.
[45] G. Subbiahdoss, R. Kuijer, H.J. Busscher, H.C. van der Mei, Mammalian cell growth versus biofilm formation on biomaterial surfaces in an *in vitro* post-operative contamination model, Microbiology 156 (2010) 3073–3078.
[46] M. Otto, *Staphylococcus epidermidis* — the 'accidental' pathogen, Nat. Rev. Microbiol. 7 (2009) 555–567.
[47] S.H. Choi, Y.S. Jang, J.H. Jang, T.S. Bae, S.J. Lee, M.H. Lee, Enhanced antibacterial activity of titanium by surface modification with polydopamine and silver for dental implant application, J. Appl. Biomater. Funct. Mater. 17 (2019), https://doi.org/10.1177/2280800019847067.
[48] F.L. Bowling, D.S. Stickings, V. Edwards-Jones, D.G. Armstrong, A.J.M. Boulton, Hydrodebridement of wounds: effectiveness in reducing wound bacterial contamination and potential for air bacterial contamination, J. Foot Ankle Res. 2 (2009) 1–8.
[49] B.S. Necula, J.P.T.M. van Leeuwen, L.E. Fratila-Apachitei, S.A.J. Zaat, I. Apachitei, J. Duszczyk, *In vitro* cytotoxicity evaluation of porous TiO2-Ag antibacterial coatings for human fetal osteoblasts, Acta Biomater. 8 (2012) 4191–4197.
[50] R.G. Contreras, H. Sakagami, H. Nakajima, J. Shimada, Type of cell death induced by various metal cations in cultured human gingival fibroblasts, Vivo (Brooklyn) 24 (2010) 513–517.
[51] A. Ince, N. Schütze, C. Hendrich, R. Thull, J. Eulert, J.F. Löhr, *In vitro* investigation of orthopedic titanium-coated and brushite-coated surfaces using human osteoblasts in the presence of gentamycin, J. Arthroplast. 23 (2008) 762–771.
[52] D.O. Kendoff, T. Gehrke, P. Stangenberg, L. Frommelt, H. Bösebeck, Bioavailability of gentamicin and vancomycin released from an antibiotic containing bone cement in patients undergoing a septic one-stage total hip arthroplasty (THA) revision: a monocentric open clinical trial, HIP Int. 26 (2016) 90–96.
[53] H.J. Busscher, V. Alt, H.C. van der Mei, P.H. Fagette, W. Zimmerli, T.F. Moriarty, J. Parvizi, G. Schmidmaier, M.J. Raschke, T. Gehrke, R. Bayston, L.M. Baddour, L. C. Winterton, R.O. Darouiche, D.W. Grainger, A trans-atlantic perspective on stagnation in clinical translation of antimicrobial strategies for the control of biomaterial-implant-associated infection, ACS Biomater. Sci. Eng. 5 (2019) 402–406.